



**HAL**  
open science

## Synthetic representation of the Galilean satellites' orbital motions from L1 ephemerides

Valéry Lainey, Luc Duriez, Alain Vienne

► **To cite this version:**

Valéry Lainey, Luc Duriez, Alain Vienne. Synthetic representation of the Galilean satellites' orbital motions from L1 ephemerides. *Astronomy and Astrophysics - A&A*, 2006, 456, pp.783-788. 10.1051/0004-6361:20064941 . hal-03784955

**HAL Id: hal-03784955**

**<https://hal.science/hal-03784955>**

Submitted on 30 Sep 2022

**HAL** is a multi-disciplinary open access archive for the deposit and dissemination of scientific research documents, whether they are published or not. The documents may come from teaching and research institutions in France or abroad, or from public or private research centers.

L'archive ouverte pluridisciplinaire **HAL**, est destinée au dépôt et à la diffusion de documents scientifiques de niveau recherche, publiés ou non, émanant des établissements d'enseignement et de recherche français ou étrangers, des laboratoires publics ou privés.

# Synthetic representation of the Galilean satellites' orbital motions from L1 ephemerides<sup>★</sup>

V. Lainey<sup>1,3</sup>, L. Duriez<sup>2,3</sup>, and A. Vienne<sup>2,3</sup>

<sup>1</sup> Royal Observatory of Belgium, 3 avenue Circulaire, 1180 Bruxelles, Belgium  
e-mail: Lainey@oma.be

<sup>2</sup> Université Lille1 IMCCE/LAL, 1 impasse de l'Observatoire, 59000 Lille, France

<sup>3</sup> Institut de mécanique céleste et de calcul des éphémérides–Observatoire de Paris, UMR 8028 du CNRS, 77 avenue Denfert-Rochereau, 75014 Paris, France

Received 31 January 2006 / Accepted 10 April 2006

## ABSTRACT

**Aims.** We aim to provide a synthetic representation of the orbital motion of Io, Europa, Ganymede, and Callisto. It corresponds to a quasi-periodic Fourier series whose arguments are integer combinations of the fundamental arguments of the dynamical system, which are also given.

**Methods.** The present series are issued from frequency analysis and digital filtering treatments. The initial samplings have been taken from a former numerical integration fit to the observations and referenced as L1 ephemerides.

**Results.** Our representation allows for the identification of all the significant perturbations in the system, which helps us to understand these orbital motions. It is also useful in other related topics: the dynamical history of the system and studies requiring us to extract only major terms to compute motions such as the rotation of the bodies.

**Key words.** ephemerides – celestial mechanics – planets and satellites: general

## 1. Introduction

To have very accurate ephemerides of the Galilean satellites Io, Europa, Ganymede, and Callisto, we built a new dynamical model leading to numerical simulations of their motions (Lainey et al. 2004a). This model has been adjusted to different kinds of observations (photographic, CCD, and mutual events) done between 1891 and 2003. Thousands of observations have been used, including the most accurate ones, issued from the mutual event campaigns (PHEMU) organized by the IMCCE, from 1985 to 1992. As a result, we have given a numerical representation that is able to produce ephemerides (Lainey et al. 2004b), referenced here as L1 ephemerides.

A numerical integration of the adjusted model was performed over 1700 years. Instead of using a numerical representation by Tchebychev polynomials, as is commonly made to interpolate between time steps, we preferred using a frequency analysis to build a quasi-periodic representation of the motions. This method was first successfully used by Carpino et al. (1987) in the case of planetary motions. Our representation has today a faithful accuracy of a few tens or so kilometers upon one century and remains definite upon more than 1700 years.

Furthermore, this synthetic form is fundamental for understanding the dynamics of the system. For example, the analytical representation of the eight main Saturnian satellites' motion (Vienne & Duriez 1995) has allowed us to discover new terms. These terms lead to a better knowledge of the evolution of the Mimas-Tethys resonance (Champanois & Vienne 1999a,b). For the Galilean satellites, a representation rather similar to the one

presented here has been used in the works of Henrard (2005a,b) dealing with the rotation of Europa and Io. The present work has also been used by Noyelles (2005) to describe the evolution of the Galilean system. More generally, a synthetic form helps to identify and understand the origin and effects of the perturbations that occur in the motion of the corresponding satellites.

At the end of the 70s, Lieske (1977) refreshed Sampson analytical ephemerides (Sampson 1921) for use in Voyager spacecraft navigation. Despite the important works done by several authors (e.g. Sagnier 1975; Vu 1982; Thuillot 1984), these ephemerides are still probably the only ones that have both an analytical model and a fit to the observations. However, the related representation suffer from a few inconsistencies: the number of parameters to fit was higher than the number of degrees of freedom, and the Laplacian libration was artificially added in the series. Recently, Lainey et al. (2004a) also pointed out that some long period terms were missing in Sampson-Lieske theory. Moreover, the representation was developed in cylindrical variables instead of the usual elliptical elements. Hence, comparison between the present work and the Sampson-Lieske series is rather difficult. The present paper provides a representation of the Galilean system. We have avoided most difficulties encountered by Sampson (1921) and Lieske (1977), thanks to numerical integration. Because the numerical integration used to simulate the satellite motions had previously been fit to the observations, its present synthetic representation can be used for ephemerides purposes. This synthetic formulation offers the advantage of describing the Galilean system over a very long time span (as long as tidal effects and long solar period terms are considered negligible).

In the present paper, we give the synthetic representation of the solution L1 and describe the method developed to

<sup>★</sup> Tables 4 to 18 are only available in electronic form at <http://www.edpsciences.org>

obtain it. This representation corresponds to trigonometric series whose arguments are integer combinations of fundamental arguments of the system:  $L_i$  (the linear parts of mean longitudes of the satellites and Sun),  $\varpi_i$  and  $\Omega_i$  (the proper modes of the pericenters and nodes), and  $\nu$ ,  $\rho$ , and  $\Psi$  (the arguments of great inequalities and resonances). First, in Sect. 2, we study the frequency spectrum of the Galilean dynamical system and characterize their short and long periods. Section 3 presents how we generated the different samplings we had to analyse. In Sect. 4 the frequency analysis algorithm we used is discussed. The next section presents the filtering technique involved in separating the long period from the short period. The last section is devoted to the synthetic representation.

## 2. Form of the spectrum

A Fourier analysis usually requires a previous spectral knowledge of the signal to determine optimal sample step size and time span. We have used routines from Duriez (1990, 2003) adapted to explore all the significant short period terms. For a given dynamical system of satellites (characterized by the satellite oblateness and mutual perturbations), these routines determine the amplitude of a given inequality  $k_i L_i + k_j L_j$ , where  $L_i$  and  $L_j$  are the linear parts of the mean longitudes of the satellites  $i$  and  $j$ , and where  $k_i$  and  $k_j$  are integers. We recall that the subscript 1 is for Io, 2 for Europa, 3 for Ganymede, and 4 for Callisto.

The computations are done at the first order with respect to the masses. In these routines, the amplitudes are in fact a function of  $z = e \exp i\varpi$  and  $\zeta = \sin \frac{1}{2} \exp i\Omega$  of each satellite ( $e$ ,  $I$ ,  $\varpi$ , and  $\Omega$  denoting, respectively, the eccentricity, the inclination, the longitude of the pericenter, and the longitude of the node). Because we only want an estimation of the amplitude of the inequality, we used the maximum values for the eccentricities and the inclinations from Ferraz-Mello (1979). We explored all the inequalities for which  $k_i$  and  $k_j$  were lower than 50 and for which  $k_i + k_j$  was lower than 8 (the maximum degree in eccentricity-inclination was then 8 because of the d'Alembert rule). We retained all the short period terms with a truncation level of one kilometer. One can find the list of those greater than 10 km in Lainey (2002). It appeared that the short period term of significant amplitude and longest period corresponds to the inequality  $L_3 - 2L_4$  (50, 2 days) and affects Ganymede. The significantly shortest short period is higher than 0.6 day.

The previous routines may also be used for the long period terms. Those involve the node and pericenter precessions (proper elements), the great inequalities  $L_1 - 2L_2 = L_2 - 2L_3 + 180^\circ$  denoted  $\nu$  in the following text, the De Haerdtl inequality  $3L_3 - 7L_4$  denoted  $\rho$ , the Laplacian libration argument  $\Psi$ , and the solar Jovicentric motion<sup>1</sup>. However, it was easier to explore these terms by a preliminary frequency analysis of L1 (without the filtering procedure described in Sect. 5.1), showing that no significant long period term exists with a period below 160 days.

## 3. Sampling

To analyse L1 ephemerides, we used exactly the same software, initial conditions and parameter values that were used in Lainey et al. (2004b). The software computes and delivers Cartesian

<sup>1</sup> As Saturn was also introduced indirectly in L1 modeling by means of the planetary ephemerides DE406, its motion should also be considered here, in particular because of its great inequality in relation to Jupiter. However, no identification introducing such frequency was possible, mainly because of the long period treatment (see Sect. 5.2).

positions and velocities of each satellite in a Jovicentric J2000 Earth mean equatorial frame. To obtain all samplings in the usual elliptical elements, we first rotated each set of Cartesian coordinates in a J2000 Jovian equatorial frame. Then, a routine was applied to shift from Cartesian to Keplerian elements. This operation was done for each data point.

## 4. Frequency analysis algorithm

The frequency analysis algorithm we used is very similar to the one used in Vienne & Duriez (1992). We only indicate the main points here; however, the reader can find more details in the cited paper. First, a FFT is performed upon the initial signal determined by the numerical integration. We retain the frequency corresponding to the highest amplitude from the FFT. This frequency is only known with the precision  $\nu_0 = \frac{\pi}{T}$ , where  $T$  is the time span of the numerical integration.  $\nu_0$  is called the fundamental frequency. Then, a fine analysis (Laskar 1993) is made in order to have the exact value of the frequency. If this frequency is separated enough from the others, the precision reaches  $1.24 \sqrt{\epsilon} \nu_0$  (with the use of the Hanning window), where  $\epsilon$  is the epsilon-machine precision of the computer. "Enough" means that the distance between two frequencies is larger than  $2\nu_0$ . In that case, the corresponding term (frequency, phase, and amplitude) is removed from the signal, and we apply the procedure again to find the next term. If, in one step of the procedure, we find a frequency separated from a previously determined one by less than  $2\nu_0$ , we put this term back in the signal to determine it again. Sometimes it is enough, and the procedure continues with the discovery of new frequencies. But, if the problem occurs again with the same term, then we determine all the previous terms again, one by one. This method was firstly used by Champeño (1999). He shows that, in some conditions, the iterative procedure eliminates the problem of the influence of one frequency on the others.

## 5. Synthetic analysis

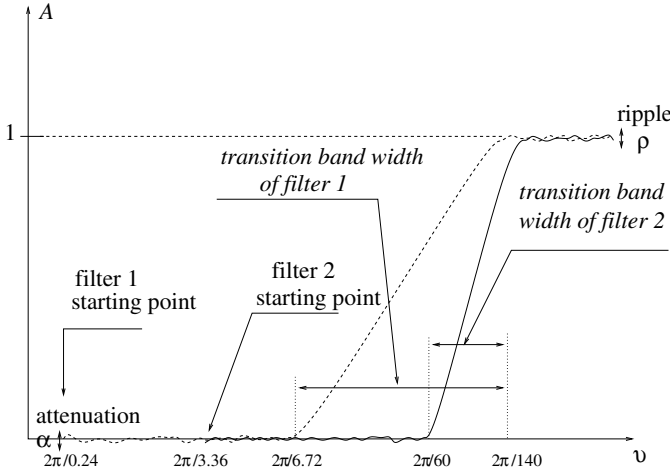
In celestial mechanics, it is usually convenient to split the orbital spectrum in two parts: the short period terms (typically a few periods) and the long period terms (few pericenter and node periods). As discussed in Sect. 2, the Galilean system spectrum has short periods that are less than a day and long periods of the order of a few centuries. So, for the practical use of the frequency analysis, it is better to cut the initial signal with respect to these two parts. This method avoids manipulating a file of several hundreds of megabytes: the time span  $T$  must be long enough to determine all the long period terms, and the step size of the signal must be small enough to determine the shortest period. We then have to use digital filtering to obtain two signals for which the sum of both is the original one. Indeed, the signal corresponding to the short period terms can be set to a much smaller time span than the original signal although the same step size can be used. The signal corresponding to the long period terms can be set with a much larger step size than the original signal, but with the same time span.

### 5.1. Digital filtering

The digital filtering used here is very similar to the one used in Duriez & Vienne (1997). The reader can find the details of the procedure in that paper. In particular, we used a two-step filtering process to avoid the use of a single filter with too high of

**Table 1.** Characteristics of the two-step filtering used to remove the short period terms from the signal in the Galilean dynamical system.

	Filter 1	Filter 2
$\Delta t$ (days)	0.24	3.36
$T_0$ (days)	6.72	60
$T_1$ (days)	140	140
$\delta t$ (days)	3.36	26.88
$2M + 1$	231	247
$\rho$	$10^{-7}$	$10^{-7}$
$\alpha$	$10^{-6}$	$10^{-6}$
$\Delta f$	0.034	0.032

**Fig. 1.** The characteristics of the two-step filtering.

a number of coefficients. Table 1 summarises the characteristics of the two filters we used. Figure 1 visualises the characteristics of the two-step filtering.  $\Delta t$  denotes the step size in input for filtering, while  $\delta t$  is the output step size;  $[T_0, T_1]$  and  $\Delta f$  are the cutting intervals expressed, respectively, in days and in sampling frequency;  $2M + 1$  is the filter length (odd number); and  $\rho$  and  $\alpha$  denote the pass-band ripple and the stop-band attenuation.

This two-step filtering method was applied at the output of our numerical integration, after converting Cartesian coordinates into Keplerian elements. To filter the mean longitude signal, we first subtracted a mean frequency empirically, and then refined it with a least squares fit. To obtain all long periodic terms, we simulated the Galilean satellites' motion over  $\pm 850$  years, starting at the Julian epoch 2 433 282.5 (January 1st, 1950, at 0h). The numerical accuracy of such integration was estimated to a few hundreds of meters. After filtering, our sample covered 1700 years with a step size of 26.88 days. This span is long enough to detect the longest periodic term of the Galilean system equal to 562 years (node of Callisto).

## 5.2. Long period treatment

To analyse the long period terms of the Galilean system, we used the frequency analysis method presented in Sect. 4 on the filtered signal. The efficiency of the quasi-periodic representation was estimated by comparing the initial signal and the reconstructed one. We obtained good results for all elements (agreement around few kilometers), except for the satellite mean longitudes (a few tens of kilometers). Problems arise because of the presence of very long solar periodic terms that cannot be analysed with only a 1700 year time span. These terms appear

in all variables, except the semi-major axis. The recognition of such terms would have needed a much longer time span, about a few hundred thousand years, because of the period of revolution of the perihelies and nodes of the planets around the Sun. With a step size as short as a day, this would also increase the numerical error in the integration process too much. Of course, these very long period terms do not appear to be periodic over 1700 years only. To overcome this problem, in all variables except the semi-major axis, we fit the residuals polluted by the very long period terms with Tchebychev polynomials. An optimal method was found in four steps. First, we filtered the residuals to remove undetected short period terms and kept only the very long period part. Then we fit the signal with low-order Tchebychev polynomials (orders less than 8). Such polynomials were then subtracted from the initial residuals, and we could start our frequency analysis treatment again. In practice, few iterations were enough to have a precision of a few tens of kilometers. Figure 2 presents all four steps of this method applied to the mean longitude of Callisto. To preserve space in this paper, these Tchebychev polynomials are not given here, but are available upon request to the authors. The long period terms found by frequency analysis in the mean longitudes (after subtracting the Tchebychev polynomials) have amplitudes greater than 2.2 km, 6.2 km, 6.1 km, and 21.8 km (respectively, in the mean longitudes of Io, Europa, Ganymede, and Callisto). This truncation level explains the precision of a few tens of kilometers that has been obtained. In other variables, we were able to obtain truncation levels half of those for mean longitudes.

## 5.3. Short period treatment

The short period spectrum is analysed by subtracting the recognized long period terms on an unfiltered sample produced by our numerical integration. We can use a much less extended time span since long periodic terms are removed. A step size of 0.24 day was used and allowed us to detect all the short period terms longer than 0.48 day. A time span of 80 years was required to separate the close frequencies of the system. We were able to adopt a truncation level of the short period terms that was less than that of long period ones (a level as low as about 0.2 km). Then, some residual long period terms were still able to be detected in the signal (at a level less than the amplitudes cited above in the long period treatment). We again used the filtering process with Tchebychev polynomials to progress in frequency analysis up to this truncation level. However, the long period terms found in this way, along with the short period ones, seem to be less reliable when trying to reconstruct their frequencies as combinations of the fundamental frequencies (see Sect. 6).

## 5.4. Precision

The trigonometric series and Tchebychev polynomials obtained by the above method represent what are called "L1 ephemerides". The corresponding tables are available by ftp<sup>2</sup>, as well as by a FORTRAN subroutine that can be used to compute ephemerides of the Galilean satellites. The subroutine output was compared to an unfiltered sampling delivered by our numerical model. The final accuracy (internal precision) over one century (centred on initial epoch 2 433 282.5) of our frequency representation was found to be of a few kilometers for Io, 20 kilometers for Europa and Ganymede, and 35 kilometers for Callisto. Over 1700 years (again centred on a J1950.0 epoch),

<sup>2</sup> ftp://ftp.imcce.fr/pub/ephem/satel/galilean/L1

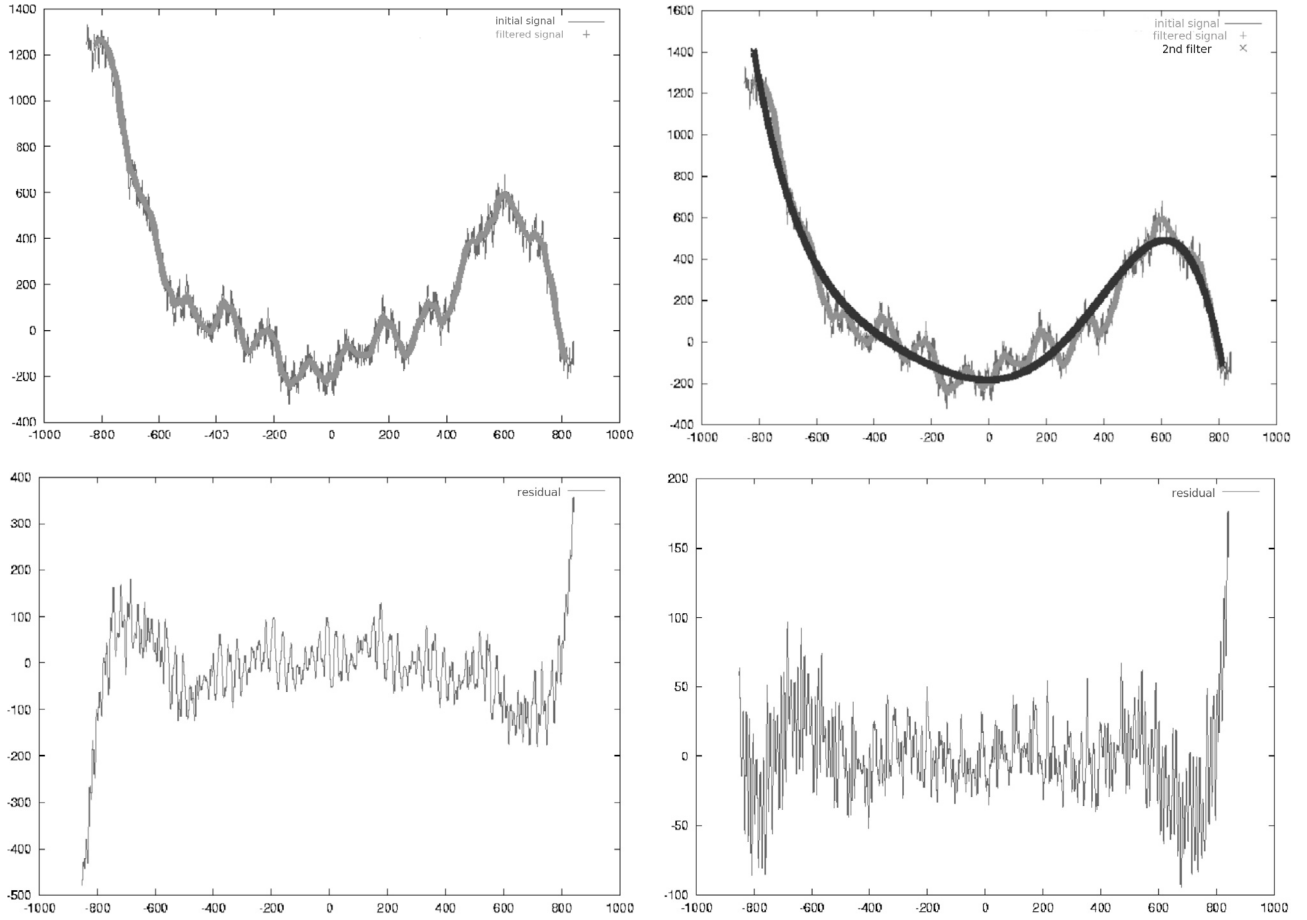


**Fig. 2.** Four step method used to reconstruct Callisto's mean longitude.  $X$ -axes are in years, and  $Y$ -axes are in kilometers. Figures on top present the residuals before the Tchebychev treatment. On the left, a filtering process is performed to remove short period terms. On the right, a Tchebychev polynomial is fit on the filtered signal. Figures on the bottom present the residuals after subtracting the Tchebychev polynomial (*left*) and applying the frequency analysis treatment again (*right*).

our representation is accurate to 25 kilometers for Io, 90 kilometers for Europa and Ganymede, and 150 kilometers for Callisto. Such accuracy is just the internal precision of our representation. The accuracy of L1 ephemerides (external precision) also introduces the error coming from the fit process (mainly due to observational errors). Considering this, the global accuracy of L1 ephemerides can be estimated to 25 kilometers for Io, 40 kilometers for Europa and Ganymede, and 55 kilometers for Callisto over one century.

## 6. Identification and synthetic representation

We first identified the fundamental arguments in the numerical representations issued from the frequency analysis process. These arguments are:

$L_i$ : the linear part in the mean longitudes of the satellite  $i$ .

$\varpi_i$ : the four proper modes in the longitudes of the pericenters.

$\Omega_i$ : the four proper modes in the longitudes of the nodes.

$\Omega_0$ : the proper mode related to the longitude of the node of the Laplacian plane.

$\nu$ : the great inequality  $L_1 - 2L_2$  or  $L_2 - 2L_3 + 180^\circ$ .

We remind the reader that  $(L_1 - 2L_2) - (L_2 - 2L_3) = L_1 - 3L_2 + 2L_3$  oscillates around  $180^\circ$ . This libration is the main effect of the Laplacian resonance.

$\Psi$ : the argument of the Laplacian resonance.

$\rho$ : the De Haerdtl great inequality  $3L_3 - 7L_4$ .

$L_S$ : the linear part, in time, in the mean longitude of the Sun.

Except  $\nu$  and  $\rho$ , which are connected to some  $L_i$ , these arguments represent the minimum set able to represent the full dynamics of the Galilean satellites.

Table 2 gives the values of these arguments and the solutions from which they issue. These solutions are given in Tables 3 to 18, where each term is in the form of a signed numerical coefficient that is supposed to be in the factor of a trigonometric function (sine, cosine, or complex exponential) whose argument corresponds to the formulae:

phase + frequency  $\times T$ ,

where  $T = \text{DJ} - 2\,433\,282.5$  (that is, the time from J1950, in days). The time scale is TDB. The short period terms are presented together with the long period ones, simply by decreasing amplitudes. These amplitudes are expressed in kilometers, by a simple conversion of AU in km in the semi-major axis, or by multiplying radians (in other variables) by the constant part of the semi-major axis (in km) of the corresponding satellite. The solutions are expressed in cosine for the semi-major axis  $a_i$ , in sine for the mean longitudes  $\mathcal{L}_i$ , and in complex exponential for the variables  $z_i$  (eccentricity-pericenter) and  $\zeta_i$  (inclination-node).

The recognition of the fundamental arguments in these solutions was possible because previous analytical works, such as

**Table 2.** Fundamental arguments of the Galilean system used for the identification. Arguments are in the form  $Phase + Frequency \times T$  with  $T = JD - 2433\,282.5$ . The argument  $\nu$  is also very close to the combinations  $L_1 - 2L_2$  and  $L_2 - 2L_3 + 180^\circ$ .

Fundamental argument	Frequency (rad/day)	Phase (deg)	Period (day)	Period (year)	Issued from solution
$L_1$	3.551552286182	82.861918	1.769	0.005	$\mathcal{L}_1$
$L_2$	1.769322711123	338.598517	3.551	0.010	$\mathcal{L}_2$
$L_3$	0.878207923589	16.467319	7.154	0.019	$\mathcal{L}_3$
$L_4$	0.376486233434	339.256972	16.689	0.046	$\mathcal{L}_4$
$L_S$	0.001450183749	318.603037	4332.938	11.863	$z_4$
$\Psi$	0.003050648672	109.319546	2059.622	5.639	$\mathcal{L}_2$
$\nu$	0.012906864147	125.663720	486.809	1.333	$z_1, z_2$ or $z_3$
$\rho$	-0.000779862000	194.603151	8056.791	22.058	$= 3L_3 - 7L_4$
$\varpi_1$	0.002664253355	25.288760	2358.328	6.457	$z_1$
$\varpi_2$	0.000677973430	157.191935	9267.598	25.373	$z_2$
$\varpi_3$	0.000127274130	121.789605	49 367.340	135.160	$z_3$
$\varpi_4$	0.000032065099	319.917125	195 950.909	536.484	$z_4$
$\Omega_1$	-0.002315096098	160.223177	2714.006	7.431	$\zeta_1$
$\Omega_2$	-0.000569206405	60.029150	11 038.500	30.222	$\zeta_2$
$\Omega_3$	-0.000124913071	191.189501	50 300.463	137.715	$\zeta_3$
$\Omega_4$	-0.000030561255	342.180346	205 593.170	562.883	$\zeta_4$
$\Omega_0$	0.000000000000	138.277188	$\infty$	$\infty$	$\zeta_4$

**Table 3.** Solution for the variable  $a_1$  (semi-major axis of Io). The series is expressed in cosine.

Amplitude (km)	Phase (deg)	Frequency (rad/day)	Identification	Freq. diff. (rad/day)	Ph. diff. (deg)
422029.958	0.00000	0.00000000000			
11.400	208.51597	3.5644591656	$2L_1 - 2L_2$	-0.155D-07	0.01083
2.706	57.04065	7.1289183312	$4L_1 - 4L_2$	-0.310D-07	0.01295
2.578	104.25820	1.7822295778	$L_1 - L_2$	-0.270D-08	0.00520
1.522	161.29083	8.9111478635	$5L_1 - 5L_2$	0.118D-07	0.02618
1.418	199.16142	8.0200331113	$3L_1 - 3L_3$	-0.235D-07	0.02238
1.379	265.54878	10.6933774362	$4L_1 - 4L_3$	0.142D-07	0.02962

that of Ferraz-Mello (1979) or of Duriez (1982) give, at least, their period. It appears that the same fundamental argument is present in several solutions, generally with very small differences (for instance  $\varpi_3$ , in solutions  $z_1, z_2, z_3$ , or  $z_4$ ). We chose the argument in one of these solutions that generally correspond to the term whose amplitude is the largest, to have the best determination of the phase (for instance  $\varpi_3$  was issued from solution  $z_3$ ).

After that, we tried to identify each frequency in the solutions as integer combinations of the fundamental frequencies. The redundancies of  $\nu$  and  $\rho$  with the relating combinations of  $L_i$  where used to identify the frequencies in the long period part of the solutions more easily.

In most cases, the frequency of each term is recognized as an integer combination of the frequencies of the fundamental arguments, by trying all possible combinations with increasing integers until the best agreement is reached, but also by respecting d'Alembert's rule (except for the solar terms, see below). As a consequence, higher integers for the arguments  $\varpi$  and  $\Omega$  corresponds to higher degree in  $z$  and  $\zeta$  (that is in eccentricities and inclinations). We then verify that the same combination of integer applied on the phases of the fundamental arguments allow us to recover the phase of the term (a difference of  $180^\circ$  was converted by changing the sign of the amplitude). Tables 3 to 18 show how each term is identified as an integer combination of the fundamental arguments. In the two last columns, we also give the difference in frequency and phase between their numerical values issued from the frequency analysis process and their evaluation by the related combination of fundamental arguments. Identification is best when the differences are smallest.

The solar terms are those depending on the argument  $L_S$ , and, to less of an extent, those with the argument  $\Omega_0$ . Generally, these terms also depend on the eccentricity and/or inclination of solar Jovicentric motion, hence on the very long period associated with the motions of the pericenter and/or node of the solar orbit. The time scale of the corresponding motion is much longer than that of the satellite. Thus, the solar frequencies of the pericenter and the node cannot be separated in our analysis. As a consequence, we can recognize a frequency close to its mean longitude frequency, but not the phase. This is why the values in column "phase difference" are not significant for solar terms and hence not given. Some other terms (essentially small terms) are not well identified; these are considered as doubtful and indicated by a star symbol (\*) in the tables. These doubtful terms come essentially from the long period part of the solution found in the short period treatment (Sect. 5.3). The given identification is considered doubtful when it corresponds to a very improbable inequality (like  $2L_S + \nu - \varpi_3 - \Omega_3$  in solution  $z_2$  or like  $2L_S - \Psi + \varpi_1 - \Omega_4$  in the mean longitude of Io) or when the difference in frequency is larger than about  $10^{-5}$  rad/day. For these terms and for the solar terms, it is better to use the numerical value of the frequency and the phase to evaluate the term instead of its doubtful identification.

In Tables 3 to 18, we have used a truncation level of 1 kilometer. There are some more terms with lower amplitudes, but they are not really significant from an analytical point of view. We recall that the internal precision of L1 is a few hundred of meters. However, we give some smaller terms that are identified, for example, as being related to the De Haerdtl great inequality or to a new, potentially interesting inequality. These

terms concern an inequality between the three last satellites:  $L_2 - 3L_3 + 2L_4$ <sup>3</sup>. This inequality of a second order of masses appears in the solution of the semi-major axis and the mean longitude of Ganymede. The corresponding amplitudes are very small (respectively, 0.36 and 4.53 kilometers), and the period is 66 days. So, it is not so far from a resonance. Can this inequality have had an influence upon the evolution of the dynamical system in the past?

More generally, thanks to the identification performed here, this synthetic representation holds some analytical information, in the sense that each term may represent a specific perturbation.

The Galilean system is sometimes referred to with two more resonances involving the arguments  $L_1 - 2L_2 + \varpi_1$  and  $L_2 - 2L_3 + \varpi_2$ . The reason is that there are librations of these arguments. However, this condition is not sufficient. If it were, such resonances should have brought two new fundamental frequencies (libration frequencies) to the system. Nonetheless, we succeeded in recognizing all frequencies as a combination of the fundamental arguments shown in Table 2. Hence, we cannot confirm the existence of such resonances.

## 7. Conclusion

We have given the trigonometric series whose arguments are integer combinations of the fundamental arguments of the dynamical system, which are also given. According to the Sampson-Lieske theory, a new representation of the Galilean orbital motions deduced from recent ephemerides is now available. It is a useful base for other dynamical studies on these satellites: the understanding, in the perturbation sense, of the orbital motions, and then the history and evolution of the dynamical system under tidal effects, as well as the rotation of the bodies. However, the doubtful identification of some terms may still be corrected. Our work to improve the frequency analysis process, to obtain better accuracy in the determination of the frequencies, is still in progress.

The present solutions benefited from L1 ephemerides, which is a former fit to the observations, recently performed in Lainey et al. (2004b). The tool is now complete and can be easily updated in light of new observations, such as spatial ones (Galileo spacecraft) or Earth-based ones (mutual events campaigns).

A FORTRAN subroutine computing L1 ephemerides by means of the present synthetic representation is available on request.

*Acknowledgements.* This work benefited from the support of the European Community's Improving Human Potential Programme under contract RTN2-2001-00414, MAGE.

## References

- Champanois, S. 1999, thesis, Observatoire de Paris
- Champanois, S., & Vienne, A. 1999a, *Celes. Mech. Dyn. Astr.*, 74, 111
- Champanois, S., & Vienne, A. 1999b, *Icarus*, 140, 106
- Duriez, L. 1982, *Celes. Mech. Dyn. Astr.*, 26, 31
- Duriez, L., & Vienne, A. 1997, *A&A*, 324, 366
- Duriez, L. 1990, *Le Développement de la Fonction Perturbatrice*. In *Modern methods in Celestial Mechanics*, ed. D. Benest, & C. Froeschlé (Éditions Frontières), 35
- Duriez, L. 2003, Maple routines for computing disturbing functions, [http://www.univ-lille1.fr/lal/mecanique\\_celeste.html](http://www.univ-lille1.fr/lal/mecanique_celeste.html)
- Ferraz-Mello, S. 1979, *Dynamics of the Galilean satellites*, ed. Universidade de Sao Paulo
- Henrard, J. 2005a, *Celes. Mech. Dyn. Astr.*, 91, 131
- Henrard, J. 2005b, *Icarus*, 178, 144
- Lainey, V. 2002, thesis, Observatoire de Paris
- Lainey, V., Duriez, L., & Vienne, A. 2004a, *A&A*, 420, 1171
- Lainey, V., Arlot, J. E., & Vienne, A. 2004b, *A&A*, 427, 371
- Laskar, J. 1993, *Physica D*, 67, 257
- Lieske, J. H. 1977, *A&A*, 56, 333
- Noyelles, B. 2005, thesis, Observatoire de Paris
- Sagnier, J. L. 1975, *Celes. Mech. Dyn. Astr.*, 12, 19
- Sampson, R. A. 1921, *Mem. R. Astron. Soc.*, 63
- Simon, J.-L., Bretagnon, P., Chapront, J., et al. 1994, *A&A*, 282, 663
- Thuillot, W. 1984, *Celes. Mech. Dyn. Astr.*, 34, 245
- Vienne, A., & Duriez, L. 1992, *A&A*, 257, 331
- Vienne, A., & Duriez, L. 1995, *A&A*, 297, 588
- Vu, D. T. 1982, *Celes. Mech. Dyn. Astr.*, 26, 265

<sup>3</sup> Not to be confused with the Laplacian resonance, which involves the three first satellites:  $L_1 - 3L_2 + 2L_3$ .

# Online Material

**Table 4.** Solution for  $\mathcal{L}_1$  (mean longitude of Io):  $\mathcal{L}_1 = L_1 +$  series expressed in sine, with  $L_1 = 1.4462132960212235 + 3.551552286182 \times T$ .

Amplitude (km)	Phase (deg)	Frequency (rad/day)	Identification	Freq. diff. (rad/day)	Ph. diff. (deg)
-81.252	282.86691	0.0135848366	$\nu + \varpi_2$	0.994D-09	-0.01125
-40.971	247.45358	0.0130341384	$\nu + \varpi_3$	-0.155D-09	-0.00026
-37.933	109.32044	0.0030506487	$\Psi$	0.363D-06	-0.00084
-23.343	85.57787	0.0129389289	$\nu + \varpi_4$	0.334D-09	0.00298
-21.253	208.61506	3.5644591050	$2L_1 - 2L_2$	0.452D-07	-0.08826
-18.756	104.25814	1.7822295778	$L_1 - L_2$	-0.270D-08	0.00526
17.644	150.95338	0.0155711172	$\nu + \varpi_1$	0.280D-09	-0.00090
15.715	122.62695	0.0014500977	$L_S$	0.860D-07	
-9.894	11.38579	0.0246753155	$2\nu + 2\Omega_2$	-0.249D-10	-0.00005
-6.766	161.59399	0.0000951962	$\varpi_3 - \varpi_4$	0.128D-07	0.27849
-5.024	57.02165	7.1289183312	$4L_1 - 4L_2$	-0.310D-07	0.03195
-4.601	66.38715	2.6733443704	$L_1 - L_3$	-0.783D-08	0.00745
3.681	131.75213	0.0004445681	$-\Omega_2 + \Omega_3$	-0.275D-06	-0.59178
3.470	48.54310	0.0005498008	$\varpi_2 - \varpi_4 + \Omega_3 - \Omega_4$	0.176D-05	-2.25913
3.181	175.58064	0.0006482675	$\varpi_2 - \varpi_3 - \Omega_3 + \Omega_4$	-0.322D-05	10.81254
-2.593	161.29048	8.9111478635	$5L_1 - 5L_2$	0.118D-07	0.02653
-2.430	199.16149	8.0200331113	$3L_1 - 3L_3$	-0.235D-07	0.02231
-2.245	85.66898	0.0029001291	$2L_S$	0.238D-06	
-2.160	265.54919	10.6933774362	$4L_1 - 4L_3$	0.142D-07	0.02921
-2.018	282.10444	0.0030554834	$2L_S - \Omega_3 - \Omega_4$	0.358D-06	*
1.923	112.21434	0.0229286259	$2\nu + \Omega_1 + \Omega_2$	0.800D-06	-0.63457
1.823	90.77307	0.0156771125	$2L_S + \nu - \varpi_3$	0.285D-05	*
1.590	132.77525	5.3466887181	$2L_1 - 2L_3$	0.708D-08	0.01395
-1.325	127.10539	0.0251554892	$-L_S + 2\nu + \varpi_2 - \Omega_4$	-0.834D-04	-19.36940
1.027	48.88513	0.0025426969	$2L_S - \Psi + \varpi_1 - \Omega_4$	0.147D-05	*

**Table 5.** Solution for the variable  $z_1$  (eccentricity and pericenter of Io). The series is expressed in complex exponentials.

Amplitude (km)	Phase (deg)	Frequency (rad/day)	Identification	Freq. diff. (rad/day)	Ph. diff. (deg)
1751.882	234.33628	-0.0129068641	$-\nu$	0.000D+00	0.00000
264.213	82.86052	3.5515522950	$L_1$	-0.880D-08	0.00140
14.887	121.78955	0.0001272742	$\varpi_3$	-0.354D-10	0.00005
8.364	319.91454	0.0000320658	$\varpi_4$	-0.652D-09	0.00258
6.179	25.28876	0.0026642534	$\varpi_1$	0.000D+00	0.00000
4.168	25.82671	-3.5773660260	$-3L_1 + 4L_2$	0.119D-07	-0.01840
-4.086	338.60240	1.7693227079	$L_2$	0.318D-08	-0.00388
-3.506	16.47338	0.8782079195	$L_3$	0.407D-08	-0.00606
2.519	290.72310	7.1160118049	$3L_1 - 2L_2$	-0.369D-06	0.66562
-2.204	157.33840	0.0006779610	$\varpi_2$	0.124D-07	-0.14646
1.964	281.56981	-5.3595956184	$-4L_1 + 5L_2$	0.293D-07	-0.02490
1.939	243.69908	-4.4684808201	$-2L_1 + 3L_3$	0.185D-07	-0.02096
-1.592	310.08529	-1.7951364446	$-L_1 + 2L_3$	0.558D-08	-0.01257
1.579	177.31174	-7.1418251641	$-3L_1 + 4L_3$	-0.983D-10	-0.02822

**Table 6.** Solution for the variable  $\zeta_1$  (inclination and node of Io). The series is expressed in complex exponentials.

Amplitude (km)	Phase (deg)	Frequency (rad/day)	Identification	Freq. diff. (rad/day)	Ph. diff. (deg)
132.609	160.22318	-0.0023150961	$\Omega_1$	0.000D+00	0.00000
38.159	60.02914	-0.0005692064	$\Omega_2$	-0.234D-10	0.00001
7.145	138.37395	0.0000000000	$\Omega_0$	0.000D+00	-0.09677
6.940	191.18949	-0.0001249131	$\Omega_3$	0.139D-11	0.00001
2.339	342.17155	-0.0000305612	$\Omega_4$	-0.905D-10	0.00880
1.513	48.64339	-0.0252445219	$-2\nu - \Omega_2$	0.127D-10	0.00002
1.021	318.58614	0.0029003681	$2L_S$	-0.646D-09	

**Table 7.** Solution for the variable  $a_2$  (semi-major axis of Europa). The series is expressed in cosine.

Amplitude (km)	Phase (deg)	Frequency (rad/day)	Identification	Freq. diff. (rad/day)	Ph. diff. (deg)
671261.171	0.00000	0.0000000000			
64.692	104.25801	1.7822295778	$L_1 - L_2$	-0.270D-08	0.00539
23.990	246.38747	2.6733443704	$3L_2 - 3L_3$	-0.782D-08	0.00612
-15.246	312.77469	5.3466887181	$3L_1 - 3L_2$	0.707D-08	0.01551
13.834	322.12913	0.8911147889	$L_2 - L_3$	-0.134D-08	0.00207
-7.834	208.51565	3.5644591656	$2L_1 - 2L_2$	-0.155D-07	0.01115
7.652	170.64578	4.4555739318	$5L_2 - 5L_3$	0.592D-08	0.01021
-4.666	56.99014	7.1289183312	$4L_1 - 4L_2$	-0.310D-07	0.06346
-4.082	161.25599	8.9111478635	$5L_1 - 5L_2$	0.118D-07	0.06102
3.474	358.71991	2.7856729212	$2L_2 - 2L_4$	0.342D-07	-0.03682
-2.712	247.45298	0.0130341383	$\nu + \varpi_3$	-0.319D-10	0.00034
2.617	94.90439	6.2378035398	$7L_2 - 7L_3$	-0.271D-07	0.01399
-1.838	265.97440	10.6933772542	$6L_1 - 6L_2$	0.196D-06	-0.39399
-1.427	85.58005	0.0129389288	$\nu + \varpi_4$	0.425D-09	0.00080
-1.270	9.82442	12.4756070797	$7L_1 - 7L_2$	-0.543D-07	0.01939
1.076	282.90788	0.0135848330	$\nu + \varpi_2$	0.456D-08	-0.05222
1.034	358.03414	4.1785094280	$3L_2 - 3L_4$	0.502D-08	-0.00951

**Table 8.** Solution for  $\mathcal{L}_2$  (mean longitude of Europa):  $\mathcal{L}_2 = L_2 +$  series expressed in sine, with  $L_2 = 0.3735263437471362 + 1.769322711123 \times T$ .

Amplitude (km)	Phase (deg)	Frequency (rad/day)	Identification	Freq. diff. (rad/day)	Ph. diff. (deg)
575.703	247.45298	0.0130341383	$\nu + \varpi_3$	-0.311D-10	0.00034
305.396	85.58002	0.0129389288	$\nu + \varpi_4$	0.426D-09	0.00083
218.089	104.25823	1.7822295778	$L_1 - L_2$	-0.270D-08	0.00517
-206.362	282.90958	0.0135848329	$\nu + \varpi_2$	0.471D-08	-0.05392
133.070	109.31960	0.0030510121	$\Psi$	0.000D+00	0.00000
123.114	122.62932	0.0014500979	$L_S$	0.859D-07	
-96.285	322.12914	0.8911147889	$L_2 - L_3$	-0.134D-08	0.00206
-51.817	246.38746	2.6733443704	$3L_2 - 3L_3$	-0.782D-08	0.00613
-42.443	150.95371	0.0155711171	$\nu + \varpi_1$	0.417D-09	-0.00123
29.990	312.77450	5.3466887181	$3L_1 - 3L_2$	0.707D-08	0.01570
29.306	208.51601	3.5644591656	$2L_1 - 2L_2$	-0.155D-07	0.01079
23.439	162.08900	0.0000298857	$-\Omega_4 + \Omega_0$	0.676D-06	-5.99217
-21.864	307.80100	0.0001249523	$-\Omega_3 + \Omega_0$	-0.393D-07	-0.71332
13.816	87.42456	0.0029001316	$2L_S$	0.236D-06	
-12.936	170.64581	4.4555739318	$5L_2 - 5L_3$	0.592D-08	0.01018
11.279	142.54854	0.0251196097	$2\nu + \Omega_2 + \Omega_3$	-0.908D-09	-0.00245
-9.507	167.20958	0.0006493040	$2L_S + 2\varpi_4 + \Omega_1$	0.976D-07	
9.446	11.38600	0.0246753155	$2\nu + 2\Omega_2$	-0.278D-10	-0.00026
8.857	57.05786	7.1289183312	$4L_1 - 4L_2$	-0.310D-07	-0.00426
7.156	305.71256	0.0030233219	$2L_S - \varpi_3 - 2\Omega_3$	-0.402D-06	
-6.982	358.71911	2.7856729212	$2L_2 - 2L_4$	0.342D-07	-0.03602
6.763	253.75671	0.0005529787	$2L_S - \varpi_4 + \Omega_1$	0.228D-06	
6.539	156.48888	8.9111510231	$5L_1 - 5L_2$	-0.315D-05	4.82813
-6.354	143.29880	0.0000934783	$-\Omega_3 + \Omega_4$	0.873D-06	7.69205
6.116	90.32784	0.0252444417	$2\nu + \Omega_2 + \Omega_0$	0.802D-07	-0.69407
-5.888	88.10350	0.0156763933	$2L_S + \nu - \varpi_3$	0.356D-05	
-5.265	333.05162	0.0259730692	$2\nu + \varpi_3 + \varpi_4$	-0.172D-08	-0.01745
-5.072	175.24631	0.0004325287	$-\Psi + \varpi_1 + \varpi_3 - \Omega_2 - \Omega_3$	0.211D-05	-28.70620 *
-4.469	112.24971	0.0229285674	$2\nu + \Omega_1 + \Omega_2$	0.858D-06	-0.66994
-4.421	106.67141	0.0260930584	$2\nu + 2\varpi_3$	-0.248D-04	28.23524 *
-3.902	94.90412	6.2378035398	$7L_2 - 7L_3$	-0.271D-07	0.01426
3.740	226.69474	0.0025481216	$\Psi - 2\varpi_3 + 2\Omega_3$	-0.148D-05	21.42465 *
-3.235	359.36045	1.3928364606	$L_2 - L_4$	0.171D-07	-0.01891
2.868	264.82632	10.6933779822	$6L_1 - 6L_2$	-0.532D-06	0.75409
2.831	77.40284	0.0030164436	$L_S + \Psi - 2\varpi_2 - \varpi_3$	0.153D-05	*
2.531	292.40619	0.0252196582	$2\nu + \Omega_2 + \Omega_4$	-0.570D-05	1.13075

**Table 9.** Solution for the variable  $z_2$  (eccentricity and pericenter of Europa). The series is expressed in complex exponentials.

Amplitude (km)	Phase (deg)	Frequency (rad/day)	Identification	Freq. diff. (rad/day)	Ph. diff. (deg)
-6282.273	234.33628	-0.0129068641	$-\nu$	0.000D+00	0.00000
200.640	338.60239	1.7693227079	$L_2$	0.318D-08	-0.00387
143.585	121.78957	0.0001272742	$\varpi_3$	-0.538D-10	0.00003
132.974	157.19194	0.0006779734	$\varpi_2$	0.000D+00	0.00000
81.249	319.93931	0.0000320566	$\varpi_4$	0.848D-08	-0.02219
56.187	92.21491	-0.9040216581	$-2L_2 + 3L_3$	0.661D-08	-0.00999
55.280	82.86051	3.5515522950	$L_1$	-0.880D-08	0.00141
-21.206	16.47324	0.8782079195	$L_3$	0.407D-08	-0.00592
-19.769	25.82779	-3.5773660260	$-3L_1 + 4L_2$	0.119D-07	-0.01948
-18.725	130.08648	-1.7951364497	$-3L_2 + 4L_3$	0.107D-07	-0.01275
9.731	167.95660	-2.6862512422	$-4L_2 + 5L_3$	0.157D-07	-0.01407
9.334	346.88341	-0.0259410024	$-2\nu - \varpi_3$	-0.191D-10	-0.00046
7.275	339.88292	-1.0163502160	$-L_2 + 2L_4$	-0.282D-07	0.03251
-5.516	281.57856	-5.3595956184	$-4L_1 + 5L_2$	0.293D-07	-0.03365
4.962	148.75621	-0.0258457929	$-2\nu - \varpi_4$	-0.465D-09	-0.00078
4.203	356.68305	-7.1418248394	$-9L_2 + 10L_3$	-0.325D-06	0.60349
-3.488	311.42179	-0.0264916967	$-2\nu - \varpi_2$	-0.500D-08	0.05883
2.920	113.06959	0.3765422106	$L_4 - 2\Omega_4 + 2\Omega_0$	0.514D-05	-1.61834
2.825	178.77781	4.4427230757	$4L_2 - 3L_3 - 2\Omega_4 + 2\Omega_0$	0.512D-05	-1.59203
2.772	243.69827	-4.4684808201	$-6L_2 + 7L_3$	0.184D-07	-0.01814
-2.483	300.73159	2.6604375002	$2L_2 - L_3$	-0.155D-08	-0.00188
-1.836	72.96507	-8.9240546532	$-6L_1 + 7L_2$	-0.860D-07	0.05304
-1.803	43.31370	0.0158069532	$2L_S + \nu - \varpi_3 - \Omega_3$	-0.208D-05	*
1.549	111.37726	7.1160114825	$7L_2 - 6L_3$	-0.462D-07	0.00844
1.353	335.08976	-2.4091843401	$-2L_2 + 3L_4$	-0.238D-05	5.48412
-1.242	153.77170	0.0006823661	$L_S - \Psi - \varpi_4 - \Omega_1$	-0.163D-06	*
1.219	149.24800	6.2248966819	$6L_2 - 5L_3$	-0.331D-07	0.00651
-1.201	328.79491	-10.7062843289	$-7L_1 + 8L_2$	0.146D-07	-0.04020
1.109	187.11938	5.3337818461	$5L_2 - 4L_3$	0.152D-07	0.00393
-1.051	354.02690	-0.0114535888	$L_S - \nu + \varpi_3 + \Omega_3 - \Omega_0$	-0.730D-06	*

**Table 10.** Solution for the variable  $\zeta_2$  (inclination and node of Europa). The series is expressed in complex exponentials.

Amplitude (km)	Phase (deg)	Frequency (rad/day)	Identification	Freq. diff. (rad/day)	Ph. diff. (deg)
2712.225	60.02915	-0.0005692064	$\Omega_2$	0.000D+00	0.00000
147.706	191.18947	-0.0001249131	$\Omega_3$	0.249D-11	0.00003
111.600	138.28257	0.0000000000	$\Omega_0$	0.000D+00	-0.00539
39.623	342.17000	-0.0000305616	$\Omega_4$	0.347D-09	0.01035
-7.050	160.22752	-0.0023150966	$\Omega_1$	0.514D-09	-0.00434
-6.910	48.64343	-0.0252445219	$-2\nu - \Omega_2$	0.137D-10	-0.00002
4.873	318.58591	0.0029003677	$2L_S$	-0.173D-09	
1.235	16.31813	-0.0014500579	$-L_S$	-0.126D-06	

**Table 11.** Solution for the variable  $a_3$  (semi-major axis of Ganymede). The series is expressed in cosine.

Amplitude (km)	Phase (deg)	Frequency (rad/day)	Identification	Freq. diff. (rad/day)	Ph. diff. (deg)
1070621.016	0.00000	0.0000000000			
208.394	66.38716	2.6733443704	$L_1 - L_3$	-0.783D-08	0.00744
96.488	322.12917	0.8911147889	$L_2 - L_3$	-0.134D-08	0.00203
34.378	74.46116	1.0034433457	$2L_3 - 2L_4$	0.346D-07	-0.04047
-18.272	284.25832	1.7822295778	$2L_2 - 2L_3$	-0.269D-08	0.00408
16.393	111.65062	1.5051650462	$3L_3 - 3L_4$	0.243D-07	-0.01958
10.493	37.22994	0.5017216696	$L_3 - L_4$	0.205D-07	-0.01959
8.196	148.92348	2.0068866946	$4L_3 - 4L_4$	0.661D-07	-0.08209
-5.904	132.77458	5.3466887181	$6L_2 - 6L_3$	0.710D-08	0.01261
-5.434	208.51658	3.5644591656	$4L_2 - 4L_3$	-0.155D-07	0.00821
4.353	115.29854	1.7535157350	$2L_3 - 2L_S$	-0.255D-06	0.43003
4.207	186.15405	2.5086083722	$5L_3 - 5L_4$	0.786D-07	-0.10232
-3.111	170.64579	4.4555739318	$5L_2 - 5L_3$	0.592D-08	0.01020
2.198	223.38618	3.0103300418	$6L_3 - 6L_4$	0.991D-07	-0.12410
-1.794	94.90455	6.2378035398	$7L_2 - 7L_3$	-0.271D-07	0.01383
1.677	247.45283	0.0130341383	$\nu + \varpi_3$	-0.839D-11	0.00049
-1.639	282.88546	0.0135848349	$\nu + \varpi_2$	0.264D-08	-0.02980
1.494	55.40543	0.6269963378	$2L_3 - 3L_4 + \varpi_4$	-0.713D-05	-0.32458
1.162	260.61772	3.5120517183	$7L_3 - 7L_4$	0.113D-06	-0.14529
1.109	9.24780	0.1253136166	$L_3 - 2L_4 + \varpi_4$	-0.461D-04	8.62270 *
...					
0.364	112.32745	0.1123285451	$-L_2 + 3L_3 - 2L_4$	0.476D-07	-0.03795

**Table 12.** Solution for  $\mathcal{L}_3$  (mean longitude of Ganymede):  $\mathcal{L}_3 = L_3 +$  series expressed in sine, with  $L_3 = 0.2874089391143348 + 0.878207923589 \times T$ .

Amplitude (km)	Phase (deg)	Frequency (rad/day)	Identification	Freq. diff. (rad/day)	Ph. diff. (deg)
247.399	122.63008	0.0014500978	$L_S$	0.859D-07	
-195.778	247.45287	0.0130341383	$\nu + \varpi_3$	-0.568D-11	0.00045
161.918	282.88704	0.0135848348	$\nu + \varpi_2$	0.276D-08	-0.03138
-124.590	246.38709	2.6733443704	$3L_2 - 3L_3$	-0.782D-08	0.00650
-102.295	85.58049	0.0129389288	$\nu + \varpi_4$	0.447D-09	0.00036
87.282	322.12912	0.8911147889	$L_2 - L_3$	-0.134D-08	0.00208
-85.780	74.46115	1.0034433457	$2L_3 - 2L_4$	0.346D-07	-0.04046
-64.989	37.23009	0.5017216704	$L_3 - L_4$	0.197D-07	-0.01974
58.233	160.01306	0.0000298809	$-\varpi_3 + \varpi_4 - \Omega_3 + \Omega_0$	-0.177D-06	-14.79786
-52.381	307.74553	0.0001249528	$-\Omega_3 + \Omega_0$	-0.397D-07	-0.65785
-45.777	104.25834	1.7822295778	$L_1 - L_2$	-0.270D-08	0.00506
-32.907	111.71745	1.5051650065	$3L_3 - 3L_4$	0.640D-07	-0.08641
-18.176	109.31254	0.0030507678	$\Psi$	0.244D-06	0.00706
16.565	326.08583	0.0006516407	$-\rho - 4\varpi_4$	-0.391D-07	-0.35748
-15.553	10.80820	0.1253082718	$L_3 - 2L_4 + \varpi_4$	-0.407D-04	7.06230 *
-14.523	160.02848	0.0005566368	$-\rho - \varpi_3 - 3\varpi_4$	-0.244D-06	3.82739
-14.416	148.92304	2.0068866946	$4L_3 - 4L_4$	0.661D-07	-0.08165
10.227	132.77449	5.3466887181	$6L_2 - 6L_3$	0.710D-08	0.01270
9.417	208.51667	3.5644591656	$4L_2 - 4L_3$	-0.155D-07	0.00812
8.079	306.87973	0.0000924270	$-2L_S + \varpi_2 - \Omega_1 - \Omega_0$	0.275D-06	*
-7.617	115.28233	1.7535157644	$2L_3 - 2L_S$	-0.285D-06	0.44624
6.868	88.95953	0.0029001310	$2L_S$	0.237D-06	
-6.769	186.15469	2.5086083722	$5L_3 - 5L_4$	0.786D-07	-0.10296
-6.056	142.44956	0.0004483462	$-L_S - \Psi + \varpi_1 - \Omega_1 + \Omega_4$	-0.754D-06	*
5.628	11.38555	0.0246753155	$2\nu + 2\Omega_2$	-0.191D-10	0.00019
5.034	170.64584	4.4555739318	$5L_2 - 5L_3$	0.592D-08	0.01015
-5.032	55.35749	0.6269971274	$2L_3 - 3L_4 + \varpi_4$	-0.792D-05	-0.27664
-4.985	206.98165	0.0004363323	$L_S + 2\Omega_2 - \Omega_3 + \Omega_0$	0.352D-06	*
-4.534	112.32691	0.1123285428	$-L_2 + 3L_3 - 2L_4$	0.500D-07	-0.03741
-4.149	129.60090	0.0251466639	$-L_S + 2\nu - \rho$	-0.326D-05	*
-3.488	325.79427	0.0017074577	$L_S - \rho - \varpi_2 - \Omega_3 - \Omega_4$	0.890D-07	*

**Table 13.** Solution for the variable  $z_3$  (eccentricity and pericenter of Ganymede). The series is expressed in complex exponentials.

Amplitude (km)	Phase (deg)	Frequency (rad/day)	Identification	Freq. diff. (rad/day)	Ph. diff. (deg)
1529.897	121.78960	0.0001272741	$\varpi_3$	0.000D+00	0.00000
825.549	319.91861	0.0000320643	$\varpi_4$	0.758D-09	-0.00149
634.441	234.33628	-0.0129068641	$-v$	0.000D+00	0.00000
219.006	302.02716	-0.1252354408	$-L_3 + 2L_4$	-0.160D-07	0.01947
191.119	16.46862	0.8782079244	$L_3$	-0.836D-09	-0.00130
121.194	82.86189	3.5515522950	$L_1$	-0.880D-08	0.00003
-70.530	130.07531	-1.7951364395	$-3L_2 + 4L_3$	0.441D-09	-0.00158
53.216	338.59968	1.7693227129	$L_2$	-0.181D-08	-0.00116
-33.873	92.20641	-0.9040216503	$-2L_2 + 3L_3$	-0.119D-08	-0.00149
30.813	264.80574	-0.6269571234	$-2L_3 + 3L_4$	-0.235D-07	0.03054
-19.458	339.25199	0.3764862399	$L_4$	-0.648D-08	0.00498
11.301	227.57993	-1.1286788041	$-3L_3 + 4L_4$	-0.329D-07	0.04600
-7.581	346.88325	-0.0259410024	$-2v - \varpi_3$	-0.840D-11	-0.00030
-7.580	160.30462	0.0006777426	$\varpi_2$	0.231D-06	-3.11268
-6.536	81.08319	-0.8753076942	$-L_3 + \varpi_1 + \varpi_3 - \Omega_3 + \Omega_0$	0.162D-04	-3.38447 *
-6.168	243.68203	-4.4684807883	$-6L_2 + 7L_3$	-0.133D-07	-0.00190
-6.136	167.94426	-2.6862512193	$-4L_2 + 5L_3$	-0.728D-08	-0.00173
5.171	155.49097	0.0027731330	$2L_S - \varpi_3$	-0.396D-07	-0.07450
4.990	190.35365	-1.6304004832	$-4L_3 + 5L_4$	-0.440D-07	0.06193
-4.084	148.75671	-0.0258457930	$-2v - \varpi_4$	-0.437D-09	-0.00128
3.745	90.90874	1.8816512921	$3L_3 - 2L_4$	0.118D-07	-0.02073
-3.222	205.81317	-3.5773660056	$-5L_2 + 6L_3$	-0.845D-08	-0.00184
-2.648	306.31315	0.2512257684	$-L_3 + 3L_4 - \varpi_3 - \Omega_3 + \Omega_4$	-0.791D-05	4.19169
2.614	269.57365	-0.2504961383	$-2L_3 + 4L_4 - \varpi_3 - \Omega_3 + \Omega_4$	-0.770D-05	3.72084
2.588	197.71646	0.0000000000	$\varpi_3 + \Omega_3 - \Omega_0$	-0.236D-05	23.01454 *
2.478	317.33703	0.0028683339	$L_S + 2\varpi_2 - 2\Omega_4$	-0.108D-05	*
2.425	318.61041	0.0014501893	$L_S$	-0.555D-08	-0.00737
2.382	153.12540	-2.1321221655	$-5L_3 + 6L_4$	-0.519D-07	0.07984
2.243	128.05821	2.3833730193	$4L_3 - 3L_4$	-0.252D-07	0.04015
-1.503	53.69648	1.3799296042	$2L_3 - L_4$	0.956D-08	-0.01881
1.278	165.36674	2.8850946416	$5L_3 - 4L_4$	0.426D-07	-0.05803
-1.197	281.55100	-5.3595955727	$-4L_1 + 5L_2$	-0.164D-07	-0.00609
1.186	115.89526	-2.6338438454	$-6L_3 + 7L_4$	-0.621D-07	0.09963
-1.110	23.33241	-0.8738575909	$-L_3 + \varpi_1 + \varpi_2 - 2\Omega_2 + \Omega_3 + \Omega_0$	0.539D-05	-7.91065 *

**Table 14.** Solution for the variable  $\zeta_3$  (inclination and node of Ganymede). The series is expressed in complex exponentials.

Amplitude (km)	Phase (deg)	Frequency (rad/day)	Identification	Freq. diff. (rad/day)	Ph. diff. (deg)
1705.791	191.18950	-0.0001249131	$\Omega_3$	0.000D+00	0.00000
913.571	138.27696	0.0000000000	$\Omega_0$	0.000D+00	0.00022
376.146	342.17492	-0.0000305610	$\Omega_4$	-0.238D-09	0.00543
-154.376	60.02914	-0.0005692063	$\Omega_2$	-0.842D-10	0.00001
16.841	318.58769	0.0029003665	$2L_S$	0.997D-09	
2.694	16.31649	-0.0014500554	$-L_S$	-0.128D-06	
2.188	101.14211	0.0014501384	$L_S$	0.454D-07	
1.921	261.09101	0.0043504622	$3L_S$	0.891D-07	
1.458	48.64347	-0.0252445219	$-2v - \Omega_2$	0.127D-10	-0.00006

**Table 15.** Solution for the variable  $a_4$  (semi-major axis of Callisto). The series is expressed in cosine.

Amplitude (km)	Phase (deg)	Frequency (rad/day)	Identification	Freq. diff. (rad/day)	Ph. diff. (deg)
1883133.534	0.00000	0.0000000000			
537.835	37.22265	0.5017216817	$L_3 - L_4$	0.851D-08	-0.01230
412.594	103.61504	3.1750660413	$L_1 - L_4$	0.114D-07	-0.01009
192.606	359.35287	1.3928364698	$L_2 - L_4$	0.785D-08	-0.01133
-62.438	74.43094	1.0034433697	$2L_3 - 2L_4$	0.106D-07	-0.01025
41.749	40.92573	0.7500722587	$2L_4 - 2L_S$	-0.159D-06	0.38214
-29.893	111.66879	1.5051650462	$3L_3 - 3L_4$	0.243D-07	-0.03775
-14.977	148.89551	2.0068867266	$4L_3 - 4L_4$	0.340D-07	-0.05412
-7.689	186.12419	2.5086084022	$5L_3 - 5L_4$	0.485D-07	-0.07246
-7.116	278.66101	0.7486221659	$2L_4 - 3L_S$	-0.250D-06	
5.210	8.64176	0.3764591707	$L_4 - \varpi_4$	-0.500D-05	10.69809
4.246	296.06433	0.1253067807	$L_3 - 2L_4 + \varpi_4 - \Omega_4 + \Omega_0$	0.870D-05	32.09690 *
-3.938	191.93984	3.0103491233	$6L_3 - 6L_4$	-0.190D-04	31.32224 *
3.577	249.65788	0.6269823880	$-L_3 + 4L_4 - L_S$	-0.696D-03	*
3.291	86.37571	2.7986109087	$L_1 - 2L_4 + \varpi_4$	0.976D-06	-2.11061
-2.560	358.71376	2.7856729335	$2L_2 - 2L_4$	0.219D-07	-0.03067
-2.124	260.58738	3.5120517575	$7L_3 - 7L_4$	0.736D-07	-0.11495
-1.795	106.47783	1.1287042579	$3L_4 - 2\varpi_2 + \varpi_4 - \Omega_2 - \Omega_0$	-0.233D-06	-1.47999
1.622	314.39993	6.7395238593	$3L_1 - 2L_2 - L_4$	0.134D-05	-2.26818
1.619	342.47195	1.0163811590	$L_2 - 2L_4 + \varpi_3 - 2\varpi_4 + \Omega_4 + \Omega_0$	0.167D-05	0.02550
...					
0.037	325.97902	0.0006516502	$-\rho - 4\varpi_4$	-0.486D-07	-0.25067
-0.028	163.85638	0.0005563954	$-\rho - \varpi_3 - 3\varpi_4$	-0.285D-08	-0.00051

**Table 16.** Solution for  $\mathcal{L}_4$  (mean longitude of Callisto):  $\mathcal{L}_4 = L_4 +$  series expressed in sine, with  $L_4 = 0.3620341291375704 + 0.376486233434 \times T$ .

Amplitude (km)	Phase (deg)	Frequency (rad/day)	Identification	Freq. diff. (rad/day)	Ph. diff. (deg)
1051.926	122.63707	0.0014500979	$L_S$	0.858D-07	
-716.686	156.75463	0.0000297297	$-\varpi_3 + \varpi_4 - \Omega_3 + \Omega_0$	-0.256D-07	-11.53943
415.260	37.23060	0.5017216724	$L_3 - L_4$	0.177D-07	-0.02025
353.633	103.61820	3.1750660413	$L_1 - L_4$	0.114D-07	-0.01325
144.421	359.35978	1.3928364637	$L_2 - L_4$	0.140D-07	-0.01824
140.681	74.46111	1.0034433457	$2L_3 - 2L_4$	0.346D-07	-0.04042
-73.126	40.84572	0.7500723697	$2L_4 - 2L_S$	-0.270D-06	0.46215
63.092	307.75076	0.0001249401	$-\Omega_3 + \Omega_0$	-0.270D-07	-0.66308
55.182	111.69205	1.5051650209	$3L_3 - 3L_4$	0.496D-07	-0.06101
35.015	83.82945	0.0029001339	$2L_S$	0.234D-06	
-32.096	325.97507	0.0006516504	$-\rho - 4\varpi_4$	-0.488D-07	-0.24672
28.509	164.72259	0.0005564607	$-\rho - \varpi_3 - 3\varpi_4$	-0.681D-07	-0.86672
-28.026	190.91569	0.1253079008	$L_3 - 2L_4 + \varpi_4 - \Omega_4 + \Omega_0$	-0.982D-05	-16.94836 *
24.467	148.92304	2.0068866946	$4L_3 - 4L_4$	0.661D-07	-0.08165
-21.866	321.95798	0.0000931663	$-L_S - \varpi_2 - \Omega_1 + \Omega_3 - \Omega_4$	-0.579D-06	*
12.469	278.25671	0.7486228617	$2L_4 - 3L_S$	-0.946D-06	
12.313	203.85907	0.0016550514	$3L_S - \varpi_1 - \varpi_4$	-0.819D-06	
11.596	186.15420	2.5086083722	$5L_3 - 5L_4$	0.786D-07	-0.10247
8.813	55.35470	0.6269971662	$2L_3 - 3L_4 + \varpi_4$	-0.795D-05	-0.27385

**Table 17.** Solution for the variable  $z_4$  (eccentricity and pericenter of Callisto). The series is expressed in complex exponentials.

Amplitude (km)	Phase (deg)	Frequency (rad/day)	Identification	Freq. diff. (rad/day)	Ph. diff. (deg)
13889.204	319.91712	0.0000320651	$\varpi_4$	0.000D+00	0.00000
389.041	339.24735	0.3764862419	$L_4$	-0.851D-08	0.00962
299.394	16.46910	0.8782079244	$L_3$	-0.836D-09	-0.00178
-293.982	121.79592	0.0001272744	$\varpi_3$	-0.283D-09	-0.00632
279.842	82.86193	3.5515522950	$L_1$	-0.880D-08	-0.00001
119.593	338.59974	1.7693227129	$L_2$	-0.181D-08	-0.00122
112.866	235.63186	-2.7985797955	$-L_1 + 2L_4$	-0.239D-07	0.02017
101.814	317.36333	0.0028683408	$2L_S - \varpi_4$	-0.384D-07	-0.07438
-92.198	264.81049	-0.6269571253	$-2L_3 + 3L_4$	-0.216D-07	0.02579
62.837	298.32179	-0.3735860173	$-L_4 + 2L_S$	0.151D-06	-0.37269
55.709	339.89402	-1.0163502275	$-L_2 + 2L_4$	-0.167D-07	0.02141
55.049	301.99244	-0.1252354245	$-L_3 + 2L_4$	-0.322D-07	0.05419
37.208	190.89675	0.0000000000	$\varpi_4 + \Omega_4 - \Omega_0$	-0.150D-05	27.07647 *
-34.565	227.58138	-1.1286788041	$-3L_3 + 4L_4$	-0.329D-07	0.04455
17.026	318.60304	0.0014501837	$L_S$	0.000D+00	0.00000
-15.439	190.35557	-1.6304004832	$-4L_3 + 5L_4$	-0.440D-07	0.06001
-11.375	80.04373	0.0043191832	$3L_S + \Omega_4 - \Omega_0$	0.807D-06	-0.33145
10.714	240.59046	-0.3721359266	$-L_4 + 3L_S$	0.244D-06	
-7.614	269.33833	-0.2504960289	$-2L_3 + 4L_4 - \varpi_4$	-0.695D-05	14.83780
-7.420	153.12774	-2.1321221655	$-5L_3 + 6L_4$	-0.519D-07	0.07750
6.949	20.17257	1.1265585019	$3L_4 - 2L_S$	-0.169D-06	0.39227
-5.377	318.57178	-0.0000315849	$\varpi_4 + \Omega_3 - 2\Omega_4 + \Omega_0$	-0.141D-06	6.45133
-5.007	14.87965	0.0014182026	$L_S - \varpi_4$	-0.839D-07	
-3.712	115.89802	-2.6338438454	$-6L_3 + 7L_4$	-0.621D-07	0.09687
3.639	294.60685	0.2512311791	$-L_3 + 3L_4 - \varpi_4$	-0.125D-04	26.77962 *
-3.516	53.67176	1.3799296163	$2L_3 - L_4$	-0.256D-08	0.00591
3.171	348.33561	0.7529452084	$2L_4 - \varpi_3 - \Omega_3 + \Omega_4$	-0.566D-05	-0.62042
-3.144	90.91586	1.8816512864	$3L_3 - 2L_4$	0.175D-07	-0.02785
3.073	262.35471	0.0014822429	$L_S + \varpi_4$	0.593D-08	
-3.043	17.27883	-0.0014180284	$-L_S + \varpi_4$	-0.902D-07	
-2.643	340.52894	-2.4091866865	$-2L_2 + 3L_4$	-0.354D-07	0.04494
-2.265	155.48788	0.0027731373	$2L_S - \varpi_3$	-0.439D-07	-0.07141
-2.214	232.51257	-0.7522178950	$-2L_4 + 2\varpi_2 - \varpi_4 + \Omega_2 + \Omega_0$	0.104D-06	1.74656
-2.034	128.14122	2.3833729650	$4L_3 - 3L_4$	0.290D-07	-0.04286
-1.904	78.66637	-3.1355655166	$-7L_3 + 8L_4$	-0.811D-07	0.11817
-1.672	289.53911	-0.5016928158	$-L_3 + L_4 + \varpi_4$	0.319D-05	-6.83233
1.670	287.32356	0.0006835386	$-\rho - 3\varpi_4$	0.128D-06	-1.67808
-1.543	356.32749	-0.3750361593	$-L_4 + L_S$	0.110D-06	
1.336	252.77931	-2.4221246132	$-L_1 + 3L_4 - \varpi_4$	-0.104D-05	2.21256
1.267	182.83092	-0.3706858488	$-L_4 + 4L_S$	0.350D-06	
1.186	77.89774	1.1251084136	$3L_4 - 3L_S$	-0.265D-06	
1.154	294.51269	7.1160095483	$3L_1 - 2L_2$	0.189D-05	-3.12397
-1.051	195.48021	-1.2539396667	$-4L_3 + 6L_4 - \varpi_4$	-0.669D-05	14.27522
1.002	202.69555	0.0057685340	$4L_S - \varpi_4$	0.136D-06	
...					
-0.892	124.01796	0.0005884547	$-\rho - \varpi_3 - 2\varpi_4$	0.293D-08	-0.24496

**Table 18.** Solution for the variable  $\zeta_4$  (inclination and node of Callisto). The series is expressed in complex exponentials.

Amplitude (km)	Phase (deg)	Frequency (rad/day)	Identification	Freq. diff. (rad/day)	Ph. diff. (deg)
7235.560	138.27718	0.0000000000	$\Omega_0$	0.000D+00	0.00000
4228.368	342.18035	-0.0000305613	$\Omega_4$	0.000D+00	0.00000
-490.458	191.18883	-0.0001249131	$\Omega_3$	0.291D-10	0.00067
62.541	318.58824	0.0029003769	$2L_S$	-0.939D-08	
9.364	16.32255	-0.0014500572	$-L_S$	-0.127D-06	
-9.306	60.02826	-0.0005692030	$\Omega_2$	-0.342D-08	0.00089
8.275	101.32342	0.0014501345	$L_S$	0.493D-07	
7.086	261.08358	0.0043504645	$3L_S$	0.867D-07	
-5.804	115.13221	0.0029313051	$2L_S - \Omega_4 + \Omega_0$	-0.376D-06	